Threedimensional wave packet studies of ozone photodissociation in the Hartley band: Converged autocorrelation functions and absorption spectra

N. Balakrishnan and G. D. Billing

Citation: The Journal of Chemical Physics **101**, 2968 (1994); doi: 10.1063/1.467609
View online: http://dx.doi.org/10.1063/1.467609
View Table of Contents: http://scitation.aip.org/content/aip/journal/jcp/101/4?ver=pdfcov
Published by the AIP Publishing

Three-dimensional wave packet studies of ozone photodissociation in the Hartley band: Converged autocorrelation functions and absorption spectra

N. Balakrishnan and G. D. Billing
Department of Chemistry, H. C. Ørsted Institute, University of Copenhagen, DK-2100 Ø Copenhagen, Denmark

(Received 14 December 1993; accepted 5 May 1994)

We report fully converged autocorrelation functions governing the photodissociation of ozone in the Hartley band, by an exact solution of the time-dependent Schrödinger equation. A local-mode representation employing hyperspherical coordinates has been used for describing the dynamics. Two different potential energy surfaces (PESs) have been employed in the present investigation, and the results showed sensitivity to the choice of the PES. Our converged calculation for $J=0$ on the Sheppard–Walker PES near quantitatively reproduced the characteristic recurrence features in the autocorrelation function obtained by Johnson and Kinsey from the experimental spectrum of Freeman *et al.* This is in contrast to previously reported three-dimensional calculations which showed a factor of 10 higher recurrence intensities compared to the experimentally derived one. The absorption spectrum, obtained as the Fourier transform of the autocorrelation function, is in excellent agreement with the experimental spectrum and exhibits the unique features seen on top of the experimental spectrum, which has caused considerable theoretical interest over recent years. Calculations on the Yamashita–Morokuma surface showed a factor of 5 higher intensity for the recurrence features, in agreement with existing three-dimensional calculations. The effect of J on the autocorrelation function has also been investigated by carrying out a calculation for $J=10$ and invoking a planar approximation. The J effect became noticeable only at a later time ($t>150$ fs) of the dissociation process and its effect on the absorption spectrum was found to be only marginal.

I. INTRODUCTION

Photodissociation of ozone in the Hartley band has attracted considerable theoretical attention in recent years.[1–8] The Hartley absorption band is characterized by an electronic transition from the ground $^1A_1$ state to the excited $^1B_2$ state which asymptotically gives rise to $O_2(^1\Delta_g)+O(^1D)$. It consists of a broad absorption band in the region 33 000–48 000 cm^{-1}.

One primary reason for the renewed theoretical interest in ozone photodissociation, particularly in the Hartley band, is the presence of weak structures with a spacing of approximately 250 cm^{-1} on top of the experimental absorption spectrum of Freeman *et al.*[9] These structures were not observed in any of the early dynamical calculations on ozone photodissociation,[1–4] in which the bending angle was frozen at its equilibrium value, but the general shape and width of the spectrum have been well reproduced by these studies. Recently, Johnson and Kinsey[5] had extracted a dipole–dipole autocorrelation function from the experimental spectrum of Freeman *et al.*[9] which showed weak recurrence features. In the wave packet description of absorption spectroscopy, this corresponds to a return of the wave packet to or near the Franck–Condon region. Since the recurrence periods were not related to any of the fundamental vibrational frequencies of ozone, the origin of these recurrence features has become a subject of much theoretical intrigue in recent times. The largest of these recurrence structures occurs at a time of 128 fs, which upon converting to frequency, roughly corresponds to the spacing between the oscillations in the spectrum.

Le Quéré and Leforestier[6,7] have recently reported autocorrelation functions during ozone photodissociation by using the wave packet approach and including the bending angle in the description. Their results showed recurrence features similar to those derived from the experiment, but recurrence intensities were approximately an order of magnitude larger than those from the experiment. An explicit propagation of the wave packet was not carried out in their study, but they computed the correlation function or the survival probability directly using a recursive residue generation (RRG) method[6] based on the Lanczos algorithm.[10,11] No satisfactory explanation has been provided for the order of magnitude difference in the recurrence intensities between the calculated and the experimentally derived correlation functions, but contributions from higher J states and/or the presence of nonadiabatic coupling with higher lying electronic states were speculated. To the best of our knowledge, there has not been any three-dimensional (3D) wave packet study reported on the photodissociation of ozone in the Hartley band in which the wave function was explicitly propagated. Furthermore, no systematic investigation has been reported till now to verify any of the speculations mentioned above. Such dynamical studies are essential in unraveling various aspects of the dissociation process and, more important, assessing the adequacy of the PESs available for the chemical process so that a realistic comparison between theory and experiment can be performed.

These observations have motivated us to undertake a detailed dynamical investigation of ozone photodissociation in the Hartley band. The purpose of the present paper is fourfold. First, to present a time-dependent wave packet method-

 0021-9606/94/101(4)/2968/10/$6.00

ology for 3D photodissociation dynamics of triatomic molecules within a local mode representation which makes use of hyperspherical coordinates; second, to use the methodology developed in this paper to investigate the photodissociation dynamics of ozone in the Hartley band with special emphasis on the convergence properties of the autocorrelation function with respect to the different grid parameters employed in the calculation; third, to examine the effect of higher J states on the correlation function and hence the absorption spectrum using a coplanar approximation for the molecule; last, to study the dynamical behavior of ozone photodissociation in the Hartley band on two PESs, with an aim of achieving more physical insight into the dynamical process.

The paper is organized as follows: Section II describes the ground vibrational state wave function calculation. The hyperspherical coordinates employed in the present formulation are described in Sec. III. A brief description of the numerical methodology employed for propagating the wave packet as well as detailed convergence tests for the correlation function are provided in Sec. IV. Converged correlation functions and absorption spectra for $J=0$ on two different PESs are presented in Sec. V. A brief discussion of the planar approximation used for the calculation with higher J as well as results of this calculation are given in Sec. VI. Section VII provides a discussion on the results and a summary of our findings is given in Sec. VIII.

II. INITIAL VIBRATIONAL STATE CALCULATION

The initial state of the photodissociating molecule is computed in the local mode coordinates R_1, R_2 and β, where R_1 and R_2 are the two local stretching coordinates and β is the local bending coordinate. The vibrational Hamiltonian in these coordinates can be expressed as

$$\hat{H}' = -\frac{\hbar^2}{M}\left[\frac{\partial^2}{\partial R_1^2}+\frac{\partial^2}{\partial R_2^2}+\frac{1}{R_1}\frac{\partial}{\partial R_1}+\frac{1}{R_2}\frac{\partial}{\partial R_2}+\frac{1}{(R_1R_2)^2}(R_1^2+R_2^2-R_1R_2\cos\beta)\frac{\partial^2}{\partial\beta^2}+\cos\beta\frac{\partial^2}{\partial R_1\partial R_2}-\sin\beta\left(\frac{1}{R_2}\frac{\partial^2}{\partial\beta\partial R_1}+\frac{1}{R_1}\frac{\partial^2}{\partial\beta\partial R_2}\right)\right]+V(R_1,R_2,\beta), \quad (1)$$

where M is the mass of one oxygen atom. The ground state potential $V(R_1,R_2,\beta)$ is taken as the Barbe, Secroun, and Jouve[12] (BSJ) potential derived from spectroscopic data. We have chosen this potential instead of the ground state surfaces corresponding to the excited PESs employed in the calculations for the following reasons: First, the BSJ potential reproduces the experimental frequencies for the first several vibrational states. Second, previous studies[3,4,6,7] had also employed the same potential for ground state wave function calculations, so that a meaningful comparison of the present results with earlier findings can be carried out. The initial wave function is expanded in a complete set with Morse wave functions for the local stretching modes and harmonic wave functions for the local bending

$$\Psi(R_1,R_2,\beta) = \frac{1}{\sqrt{R_1R_2}}\sum_n^N\sum_m^M\sum_l^L C_{n,m,l}\phi_n(R_1)\phi_m(R_2)\psi_l(\beta), \quad (2)$$

where $\{\phi\}$ are the Morse wave functions and $\{\psi\}$ are the harmonic functions. The volume element for the normalization of the wave function is $R_1R_2dR_1dR_2d\beta$. The expansion coefficients $C_{n,m,l}$ are obtained by solving the time-independent Schrödinger equation

$$\hat{H}'\Psi = E_i\Psi, \quad (3)$$

where the index i collectively refers to the quantum numbers (n,m,l). The converged ground state energy of 1459 cm^{-1} from this calculation [which required $N=M=6$, and $L=8$ in the expansion in Eq. (2)] is in excellent agreement with the experimental ground state energy of 1457 cm^{-1}. Our calculation also reproduced the energies of the first several excited vibrational states within a few cm^{-1}.

III. HYPERSPHERICAL COORDINATES

Once the expansion coefficients are known, the wave function can be computed in the coordinate system in which dynamical calculations are being performed. The hyperspherical coordinates (ρ,θ,ϕ) employed in the present study are a slightly modified version of Johnson's coordinates.[13] In terms of these, the local mode coordinates can be expressed as

$$R_1 = \rho(b+a\sin\theta\cos\phi-\tfrac{1}{2}\sin\theta\sin\phi)^{1/2} \quad (4)$$

$$R_2 = \rho(b+a\sin\theta\cos\phi+\tfrac{1}{2}\sin\theta\sin\phi)^{1/2} \quad (5)$$

$$\cos\beta = -\frac{a+b\sin\theta\cos\phi}{[(b+a\sin\theta\cos\phi)^2-(1/4)\sin^2\theta\sin^2\phi]^{1/2}} \quad (6)$$

where a and b are constants related to mass scaling

$$a = \frac{d^2}{8}-\frac{1}{2d^2} \quad (7)$$

and

$$b = \frac{d^2}{8}+\frac{1}{2d^2} \quad (8)$$

with $d=\sqrt{2M/3\mu}$, where the hyperspherical reduced mass μ is defined as

$$\mu = \frac{M}{\sqrt{3}}. \quad (9)$$

The hyperangles vary in the range $0\leq\theta\leq\pi/2$ and $0\leq\phi\leq2\pi$. Thus, it can be seen from Eqs. (4)–(6) that the symmetry of the molecule is built into the model which treats the two local stretching modes equivalently. The volume element for the above transformation is

$$R_1R_2dR_1dR_2d\beta=\frac{\rho^3}{4}\sin\theta\, d\rho\, d\theta\, d\phi. \tag{10}$$

The Hamiltonian in these coordinates can be written as[14]

$$\hat{H}=\hat{H}_0+\hat{H}_1, \tag{11}$$

where

$$\hat{H}_0=-\frac{\hbar^2}{2\mu}\left[\frac{\partial^2}{\partial\rho^2}+\frac{4}{\rho^2}\left(\frac{\partial^2}{\partial\theta^2}+\frac{1}{\sin^2\theta}\frac{\partial^2}{\partial\phi^2}\right)\right]+\Delta V(\rho,\theta)+V(\rho,\theta,\phi) \tag{12}$$

and

$$\hat{H}_1=\frac{1}{\mu\rho^2}\left(\frac{\hat{J}_x^2}{1-\sin\theta}+\frac{\hat{J}_y^2}{1+\sin\theta}+\frac{\hat{J}_z\{\hat{J}_z+4i\cos\theta\hbar[\partial/(\partial\phi)]\}}{2\sin^2\theta}\right). \tag{13}$$

The extra potential $\Delta V(\rho,\theta)$ is given by

$$\Delta V(\rho,\theta)=-\frac{\hbar^2}{2\mu\rho^2}\left(\frac{1}{4}+\frac{4}{\sin^2 2\theta}\right). \tag{14}$$

For $J=0$, the $\hat{H}_1$ part of the Hamiltonian vanishes and we get a 3D problem in (ρ,θ,ϕ).

IV. NUMERICAL IMPLEMENTATION

A. Wave packet propagation

To follow the photodissociation dynamics in the time-dependent picture, one time evolves an initial wave function which is an eigenfunction of the ground state Hamiltonian under the influence of the excited state Hamiltonian. The initial wave function on the excited surface is obtained by the action of the transition dipole moment operator on the ground state wave function. Since the exact form of the transition dipole moment operator is not known for ozone, we considered it as a constant, unity, in all calculations presented here. Previous studies had also assumed a constant transition dipole moment. The role of the dipole moment becomes more important if the spatial extent of the ground state wave function is large, which is not the case with the present system.

Propagation of the wave packet was accomplished using the Lanczos method[10,11] together with the fast Fourier transform (FFT) algorithm[15] to compute second derivatives of the wave function. We have used a variable order Lanczos scheme in which the number of Lanczos recursions was altered at different time steps by comparing the magnitude of the last few recursion vectors with a predetermined accuracy parameter.

A usual problem in using hyperspherical coordinates is the presence of singularities in the Hamiltonian such as the one at $\theta=0$. This can be extremely troublesome in certain cases, particularly if the initial wave function extends to this region. In the present case, this is not a severe problem as the initial wave function along the θ grid is centered near $\theta=0.9$ rad and the dissociation involves motion of the wave packet towards larger θ angles. One usual way to remove the singularities is by shifting the grid points by half the grid spacing, so that the grid points in the shifted grid lie midway between the grid points in the original grid. Though we have adopted this procedure for the θ grid, it is possible to build up finite probability near the singularities during the course of the propagation and cause numerical problems. This is circumvented by using a sine transform instead of the usual FFT, while evaluating the second derivative of the wave function along this coordinate as a sine transform in θ in the range $0-\pi$ results in a function which is zero at the grid point 0. We achieved this by a forced sine transform in which the θ grid was extended from the range $0-\pi/2$ to $0-\pi$ such that the resulting wave function became an odd function about $\theta=\pi/2$. Performing a usual FFT on this extended grid is equivalent to a sine transform, and by construction, the wave function will be zero at $\theta=0$ and neighboring points. This procedure increased the memory as well as central processing unit (CPU) requirement by a factor of 2, but ensured a stable propagation. To prevent the dissociated wave packet from reaching the end of the ρ grid and undergoing artificial reflection, we have placed an absorbing potential beyond $\rho=3.72$ Å to absorb them. A linear negative imaginary potential similar to the one employed by Neuhauser and Baer[16] has been used for this purpose.

B. Symmetry considerations

Symmetry considerations can often greatly reduce the numerical work involved in actual calculations. This is particularly relevant in the present case as the molecule is fully symmetric with respect to the exchange of any two oxygen atoms, and hyperspherical coordinates are specially suited for describing such systems as it handles all the arrangement channels equivalently. Of the three hyperspherical coordinates, ρ defines the overall size of the system, whereas θ and ϕ together determine the shape of the molecular triangle formed by the three atoms. The arrangement channels (the different O_2+O channels) depend only on the ϕ angle, also known as the kinematic angle, and going from one arrangement channel to another involves only a simple rotation along this coordinate, referred to as a kinematic rotation. For the present system, all the three arrangement channels are equivalent and indistinguishable in the ϕ range $0-2\pi$. This is illustrated in Fig. 1, where we have plotted the Sheppard–Walker (SW) $^1B_2$ potential as a function of ϕ for fixed values of ρ and θ. As can be seen, it displays a periodicity of $2\pi/3$ (and an even symmetry within each period). This periodicity can be nicely exploited while using the FFT algorithm to compute the Laplacian of the wave function along this coordinate, thereby reducing the ϕ grid to $2\pi/3$ rad. This decreases the storage requirements by a factor of 3 and allows us to use a much denser grid in actual numerical implementations. The initial wave function when computed on the grid is centered at $\phi=0$ and is symmetrical in the range $(-\pi/3,\pi/3)$ about $\phi=0$ suggesting that a ϕ range of $-\pi/3\leq\phi\leq\pi/3$ is equivalent to using the full range $0\leq\phi\leq2\pi$. This has been also verified by performing actual calculations, which will be discussed during the convergence tests below.

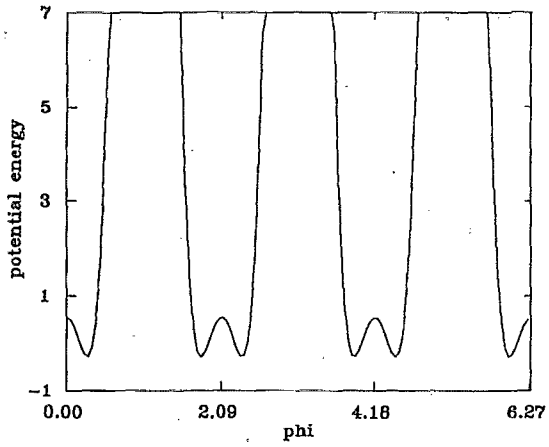

FIG. 1. The SW $^1B_2$ potential as a function of the hyperangle ϕ for fixed values of ρ and θ. Potential energy values are in ϵ units with $1\epsilon=100$ kJ/mol.

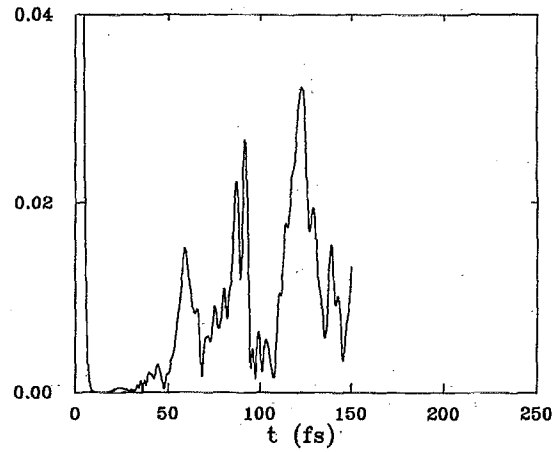

FIG. 2. The modulus of the autocorrelation function as a function of time, computed on the SW PES for $J=0$ using a grid of (81,64,48) in (ρ,θ,ϕ) with ϕ in the range $-\pi/3\leq\phi\leq\pi/3$.

C. Grid parameters and convergence tests

In order to have a correct representation of the wave function at all times during the photodissociation process, careful consideration has to be given while choosing the grid parameters. The large reduced mass of the molecule and the relatively high energy (≈2 eV) involved in the dissociation process make the ozone photodissociation an extremely challenging problem to study quantum mechanically. The grid has to be sufficiently dense along all directions to accommodate the kinetic energy released during the dissociation process. Since there is no *a priori* way of assigning the grid spacing for the angular coordinates, we had to perform a number of calculations by systematically increasing the grid sampling until convergence was attained. The ρ grid spacing can be assigned by considering the maximum energy released during the dissociation process, as it is more like a translational coordinate. However, we have performed separate calculations to ensure convergence along all the three grid directions. In the following, we illustrate this under separate titles.

D. Convergence with respect to ρ

First, we shall establish the convergence along ρ, and subsequently, ϕ and θ. We have chosen the spacing of the ρ grid *a priori* using the relation

$$\Delta\rho=\frac{\pi}{k_{\max}}, \tag{15}$$

where $k_{\max}=\sqrt{2\mu\Delta E}/\hbar$ with ΔE (taken to be 2 eV as in Ref. 7) being the energy involved in the dissociation process. We have choosen $\Delta\rho$ to be 0.03 Å, slightly smaller than that estimated from the above relation. The number of grid points along $\rho(N_\rho)$ was taken to be 81 with ρ ranging from 1.8–4.2 Å. A test calculation was carried with $\Delta\theta=\pi/128$ and $\Delta\phi=\pi/72$ rad with θ and ϕ in the range $0\leq\theta\leq\pi/2$ and $-\pi/3\leq\phi\leq\pi/3$, respectively. The number of grid points along θ and ϕ (N_θ,N_ϕ) were fixed at (64,48). In Fig. 2, we show the autocorrelation from this calculation up to 150 fs. The time step used for the propagation is 0.2 fs which required about seven to nine Lanczos iterations. To examine the convergence with respect to ρ, we carried out another calculation by decreasing N_ρ to 64 and increasing the $\Delta\rho$ to 0.035 Å. All other parameters were kept the same. The correlation function from this calculation was found to be nearly identical to the one shown in Fig. 2 and hence it is not reproduced here. Thus in our subsequent calculations, we used $N_\rho=81$ and $\Delta\rho=0.03$ Å.

E. Convergence with respect to ϕ

After the convergence along ρ was established, we increased N_ϕ to 64 and correspondingly decreased $\Delta\phi$ to $\pi/96$ rad to seek convergence along ϕ. Thus $\Delta\phi$ was defined to be

$$\Delta\phi=\frac{2\pi}{3N_\phi}, \tag{16}$$

so that the length of this grid became $2\pi/3$ in the range $(-\pi/3,\pi/3)$. The θ grid was taken to be the same as above. The autocorrelation function obtained from this calculation is shown in Fig. 3, and it is considerably different from the one shown in Fig. 2, indicating that the latter is not converged with respect to the grid spacing in ϕ. Thus we carried out another calculation by increasing N_ϕ to 96 and redefining $\Delta\phi$ according to Eq. (16). The correlation function from this calculation remained practically the same as the one obtained above, and hence we used an intermediate value of 81 for N_ϕ in the rest of our calculations. It may also be mentioned that we have carried out additional calculations to ensure that reducing the ϕ range from $(0-2\pi)$ to $(-\pi/3,\pi/3)$ did not cause any deleterious effects. This was done by performing a separate calculation using the actual ϕ range $(0-2\pi)$. In this calculation we have used $N_\phi=162$ and $\Delta\phi=\pi/81$ rad. The correlation function from this calculation was also very similar to that shown in Fig. 3. This clearly demonstrates that the results are insensitive to the choice of the ϕ range, as it should be.

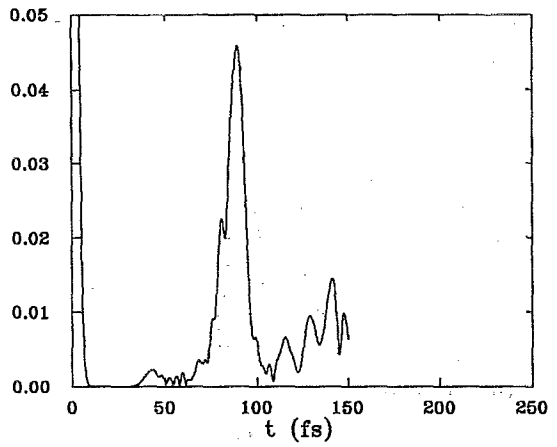

FIG. 3. The same as in Fig. 2, but using the grid (81,64,64) in (ρ,θ,ϕ).

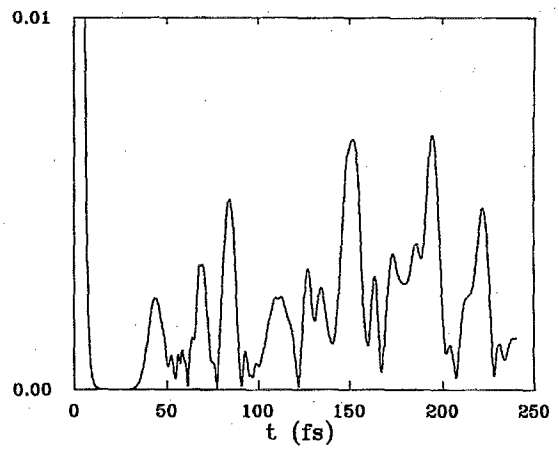

FIG. 4. Converged autocorrelation function for $J=0$ on the SW PES obtained using the grid (81,96,81) in (ρ,θ,ϕ).

F. Convergence with respect to θ

Having established the convergence along ρ and ϕ, we now pay our attention to the θ coordinate. Thus we performed a calculation by increasing N_θ to 81 and concommittantly decreasing $\Delta\theta$ so that the physical extension of the grid remained the same as before. Other grid parameters were retained at their previous values. The correlation function from this calculation exhibited a significant damping of the oscillations compared to the one shown in Fig. 3, indicating the necessity of having a very dense grid along the θ coordinate. However, yet another calculation was necessary to establish the convergence with respect to this coordinate. This was carried out by increasing N_θ to 96. The correlation function computed on this grid remained nearly identical to the one obtained above, demonstrating that further reduction in grid spacing was not necessary. The result of this calculation for the first 240 fs of the dynamics is shown in Fig. 4, and it is fully converged with respect to all grid parameters up to 150 fs. It must be mentioned that these test calculations have been rather expensive and required many hours of supercomputer time.

V. $J=0$ CALCULATIONS

A. Dynamics on the SW PES

All the convergence tests reported above have been carried out on the $^1B_2$ PES of Sheppard and Walker (SW)[2] and for $J=0$. This was constructed from the *ab initio* potential energy values of Hay *et al.*[1] combined with available experimental informations. Most of the dynamical calculations[2–7] till date on ozone photodissociation in the Hartley band have been carried out on this $^1B_2$ surface. The converged autocorrelation function computed on this surface presented in Fig. 4 exhibits a sharp initial decay, followed by a series of recurrences of intensity less than 1% of the initial value. As mentioned in the Introduction, these recurrences correspond to successive returns of the wave packet to the initial Franck–Condon region, which we shall illustrate in Sec. VII. The major recurrence features occur at 44, 69, 84, 128, 151, and 194 fs. For comparison, the correlation function obtained by Johnson and Kinsey[5] from the experimental absorption spectrum of Freeman *et al.*[9] is shown in Fig. 5. The predominant recurrence features in the experiment correlation function appear at $t=19$, 41, 68, 99, and 128 fs. The most striking aspect of this comparison is the similarity between the two correlation functions during the initial stages of the dissociation process. There is a good agreement between the locations of some of the early features, particularly, the ones at 44, 69, and 128 fs. Another important point to be mentioned is the good agreement in the magnitude of the recurrence features in the computed and the experimental correlation functions. This agreement should not be considered as fortuitous as the present results are obtained after performing comprehensive and systematic convergence tests. This is particularly relevant in the light of an order of magnitude discrepancy observed in this regard in previous stud-

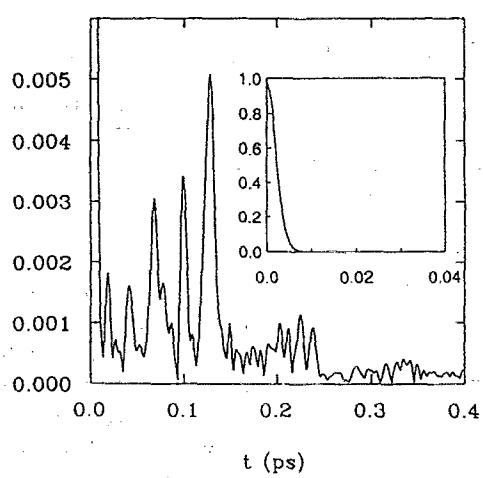

FIG. 5. Experimentally derived autocorrelation function (from Ref. 5). The initial decay is shown in the inset.

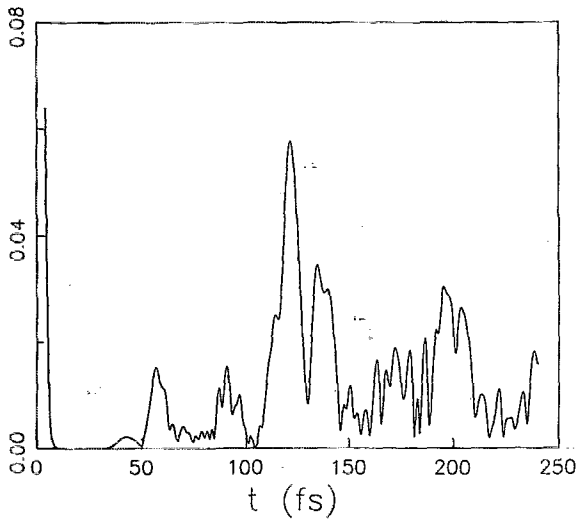

FIG. 6. The same as in Fig. 2, but using the grid (81,64,128) in (ρ,θ,ϕ) with ϕ in the range $(0\leq\phi\leq 2\pi)$.

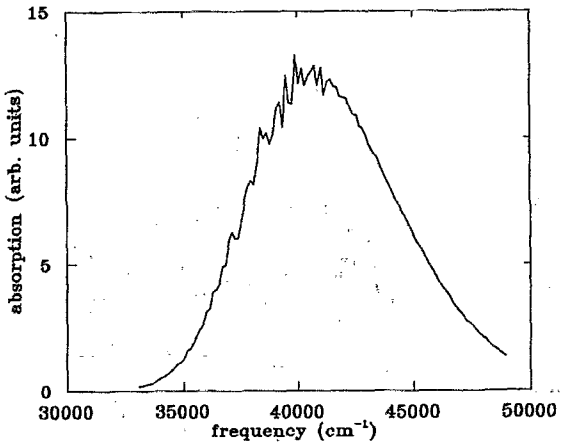

FIG. 7. The absorption spectrum as a function of radiation frequency, computed as the inverse Fourier transform of the correlation function shown in Fig. 4.

ies on the same PES by Le Quéré and Leforestier[6,7] who used the RRG method to compute the correlation function. However, it may be interesting to point out that our initial calculations have produced a correlation function which was in reasonably good agreement with that reported in Refs. 6 and 7. For example, the correlation function shown in Fig. 6 is obtained from a (81,64,128) grid in (ρ,θ,ϕ) (in this calculation, ϕ was taken in the range $0-2\pi$), and this is very similar to that reported in Ref. 7, both in terms of the recurrence positions and recurrence intensities. However, our convergence tests clearly show that the correlation function presented in Fig. 6 is not fully converged.

The total absorption cross section in the time-dependent formalism is obtained as the Fourier transform of the time-correlation function. Following Heller,[17] this can be expressed as

$$\sigma(\omega)=C\omega\int_{-\infty}^{\infty}\exp(iEt/\hbar)\langle\Phi(t=0)|\Phi(t)\rangle dt, \qquad (17)$$

where C is a constant, E the total energy, and ω the frequency of the exciting radiation such that $E=\hbar\omega+E_0$ with E_0 being the energy of the ground vibrational state. $\Phi(t)$ is the wave function evolving on the $^1B_2$ state.

The total photodissociation cross section obtained from the correlation function shown in Fig. 4 is plotted as a function of ω in Fig. 7. The experimental absorption spectrum of Freeman *et al.*[9] is shown in Fig. 8 for comparison. The maximum of the computed spectrum occurs at a higher energy due to the inaccuracy in the computed vertical energy separation between the ground and excited surfaces.[1,2] However, this is only a constant shift and has no effect on the characteristics of the spectrum. There is nearly perfect agreement between the two spectra with regard to most of the features. The important point to be mentioned is the correct reproduction of the unusual oscillations on top of the experimental spectrum, which in previous studies had either been elusive due to lack of recurrence in the correlation function[4] or too pronounced due to too much recurrence[7] (it may be worth pointing out that the spectrum reported in Ref. 7 has been obtained by rescaling the recurrent part of the correlation function, so that the magnitude of the largest recurrence coincided with the experimental counterpart). To the best of our knowledge, this is the first theoretically computed Hartley absorption spectrum of ozone which has reproduced so well all the features in the experimental spectrum. It is worth reiterating that this agreement forms a drastic test to the quantum mechanical description of molecular processes and should be regarded as another instance of our ability to predict observed phenomena from first principles.

B. Dynamics on the YM PES

Recently, Yamashita and Morokuma (YM)[8] have computed new PESs for the $^1A_1$ and $^1B_2$ states of ozone. The new

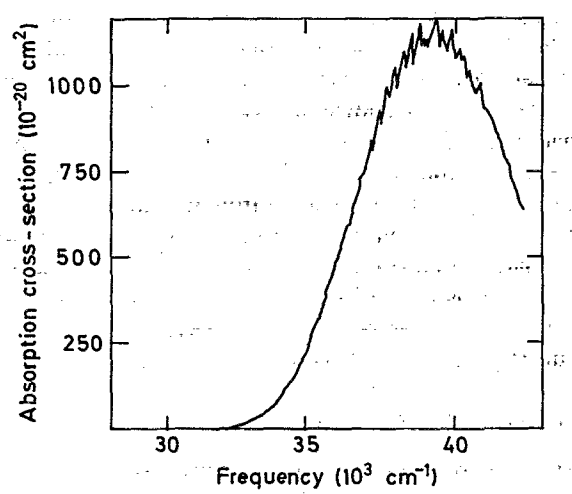

FIG. 8. Experimental absorption spectrum of Freeman *et al.* (from Ref. 9).

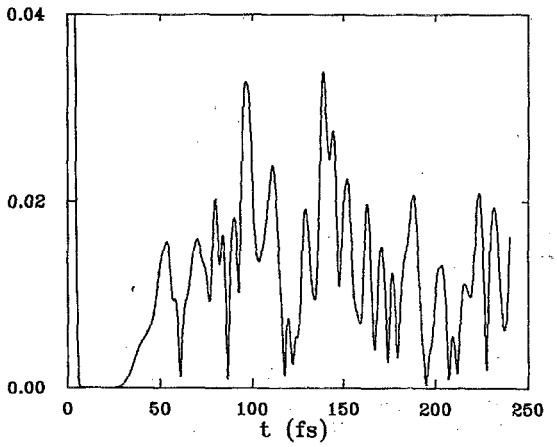

FIG. 9. The same as in Fig. 4, but on the YM surface.

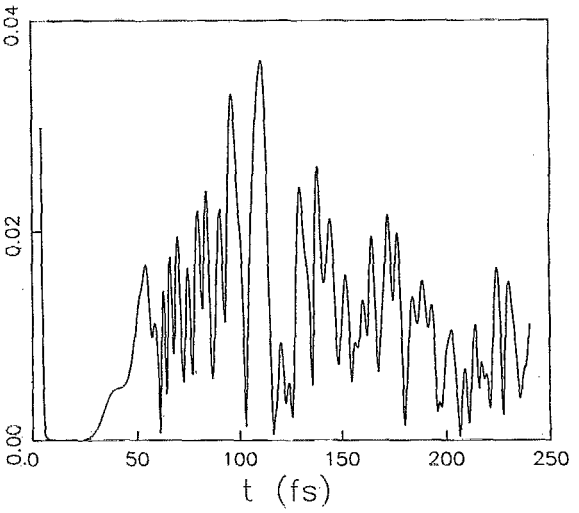

FIG. 10. The same as in Fig. 6, but on the YM surface.

$^1B_2$ PES has the correct C_s symmetry at the minima in the exit channels compared to C_{2v} for the corresponding SW PES, and the *ab initio* values used for fitting the former were claimed to be more accurate than that of the latter. The fitting procedure for both surfaces have used similar analytical formulas.

The correlation function for $J=0$ on the YM surface is presented in Fig. 9. Predominant early recurrence features arise at $t=53.6$, 96, and 139 fs, although several other narrow oscillations of comparable intensity are seen. Though some of the recurrences appear at the same time as in the SW PES, there is considerable discrepancy regarding the magnitudes of the correlation functions. The interesting, and at the same time curious aspect here is that this surface shows an entirely different convergence property compared to the SW PES. The correlation function shown in Fig. 9 is obtained using the grid which gave converged correlation function on the SW PES. In Fig. 10, we show a correlation function on the YM surface which used the same grid as the one used for obtaining the correlation function in Fig. 6, i.e., (81,64,128) in (ρ,θ,ϕ) with ϕ in the range $(0-2\pi)$. The difference between Figs. 9 and 10 is only minor as the magnitude as well as locations of most of the peaks are the same. This shows that the YM surface exhibits faster convergence with respect to the angular grids. It is also worth mentioning that the correlation function shown in Fig. 9 is very well comparable to that obtained by Yamashita *et al.*[8] using the RRG method. However, the computed correlation function on the YM surface is in considerable deviation from the experiment. This is further pronounced in the spectrum shown in Fig. 11, which shows large oscillations compared to the experimental as well the one on the SW surface. However, a detailed examination of specific properties of the potential responsible for this discrepancy lies beyond the scope of the present paper.

VI. $J\neq 0$ CALCULATIONS

The experimental absorption spectrum of Freeman *et al.*[9] was recorded at a temperature of 195 K, which corresponds to approximately $J=10$. Thus, it would be worthwhile to compute the correlation function for this value of J to examine its effect, if any, on the recurrence pattern. A full quantum mechanical study of this becomes a four-dimensional problem as $\hat{H}_1$ in Eq. (11) is no longer zero. For the present system, this is a formidable task and we have resorted to a planar approximation which is obtained from the semiclassical equivalent of the Hamiltonian presented in Eq. (11). The semiclassical Hamiltonian in hyperspherical coordinates can be expressed as[14,18]

$$\hat{H}^{sc}=\hat{H}_0+\hat{H}_1^{sc}, \tag{18}$$

where $\hat{H}_0$ is same as before and $\hat{H}_1^{sc}$ is given by

$$\hat{H}_1^{sc}=\frac{P_\gamma\{P_\gamma+4i\hbar\cos\theta[\partial/(\partial\phi)]\}}{2\mu\rho^2\sin^2\theta}+\frac{P_J^2-P_\gamma^2}{\mu\rho^2\cos^2\theta}\times(1+\sin\theta\cos 2\gamma), \tag{19}$$

where γ refers to one of the Euler angles (the other two Euler angles α and β do not appear here as the external coordinates

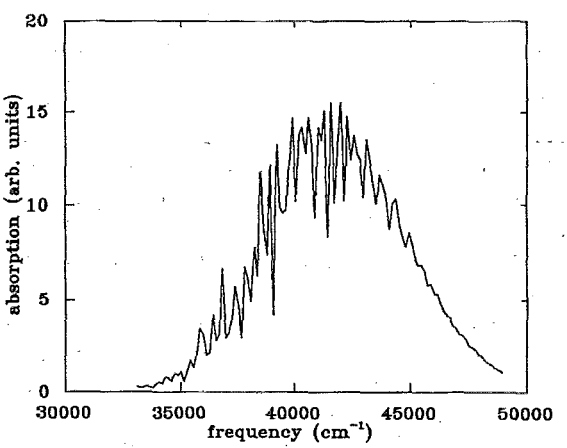

FIG. 11. The same as in Fig. 7, but on the YM surface.

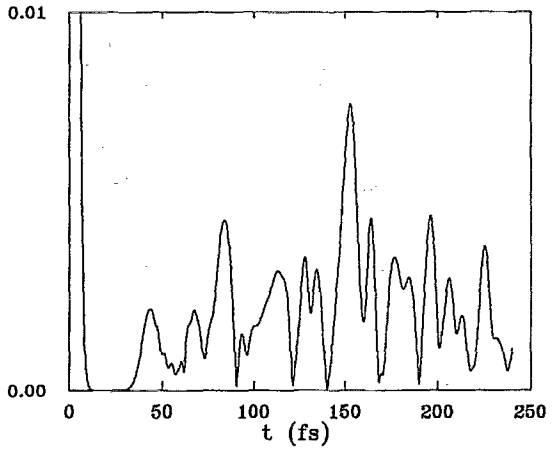

FIG. 12. The same as in Fig. 4, but for $J=10$.

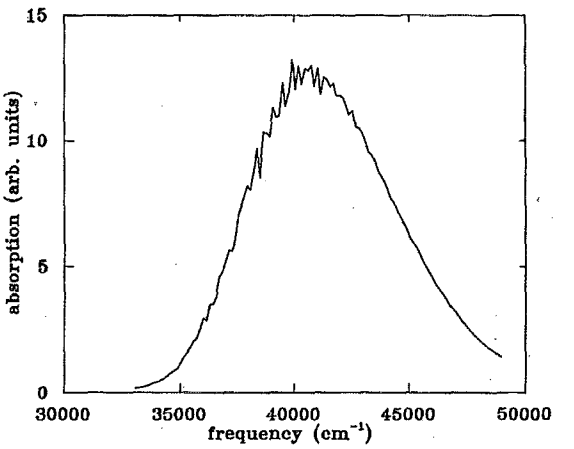

FIG. 13. The same as in Fig. 7, but for $J=10$.

are chosen to make their conjugate momenta constants of motion). Now, we obtain the planar case by making the substitution $P_J=P_\gamma$ which results in the cancellation of the second term in Eq. (19). This makes the method exact as P_γ is a constant in this case. Only for the nonplanar situations ($P_\gamma \neq P_J$) does one need to propagate γ (classically). Thus, propagating the wave function within this planar approximation is no more difficult than for $J=0$, as it costs only the additional inverse Fourier transform operation required for evaluating the first derivative of the wave function with respect to ϕ. In Fig. 12 we show the correlation function from the calculation with $J=10$ on the SW PES which is quite similar to the one for $J=0$ for the first 150 fs. The J effect seems to be operating only for times greater than this where a noticeable quenching of the oscillations can be seen. The spectrum from this calculation, shown in Fig. 13, is also nearly identical to that from the $J=0$ calculation, except that the oscillations have slightly diminished in intensity. Thus we have the important conclusion that the planar dynamics for $J=10$ is very similar to that of the full 3D dynamics for $J=0$.

Results of similar calculations on the YM surface were also in accordance with the above finding. These observations, coupled with the fact that $J=10$ corresponds to the maximum of the Boltzmann distribution at 195 K, imply that higher J values are unlikely to influence the results. Furthermore, as the spectrum on the SW PES for $J=0$ is already in good agreement with the experimental spectrum, any necessity for performing additional calculations by relaxing the restriction $P_\gamma=P_J$ is not felt, and such calculations are not expected to change the results—at least for the system investigated here.

VII. DISCUSSION

Johnson and Kinsey had carried out a detailed study of the recurrences through classical trajectory calculations on the SW $^1B_2$ PES. They have observed trajectories returning to the Franck–Condon region and have provided some explanation for the recurrence features in the correlation function. They explained the recurrences at $t=41$, 68, 99, and 128 fs in their correlation function due to families of unstable trajectories returning to the Franck–Condon region. However, no explanation has been provided towards the origin of the peak at 19 fs.

An attractive feature of the time-dependent study such as the present one is that it is possible to extract important physical insight into the dynamics by examining snapshots of the wave packet during the course of its dynamical evolution. In Figs. 14(a)–14(f) we present a few such pictures on the SW PES for $J=0$ in the form of probability density contours as a function of the two hyperangles. For convenience of plotting, the hyperradius has been integrated out. Figure 14(a) shows the initial wave packet on the upper PES, whereas Figs. 14(b)–14(f) show the wave packet at $t=20$, 40, 60, 80, and 120 fs, respectively. Though these figures are self-explanatory, they are worth some comments. Figure 14(b) shows that the wave packet is far away from the Franck–Condon region at 20 fs, and the possibility of any overlap with the initial wave function does not arise. This is also reflected in the correlation function depicted in Fig. 9. So the origin of the peak at 19 fs in the experimentally derived correlation function appears to be unexplainable. Another point to be mentioned is that the motion of the wave packet out of the Franck–Condon region does not immediately lead to dissociation as the activity along θ is very small in the initial stages of the dynamics. However, a very strong activity is seen along the ϕ coordinate, suggesting the involvement of both the bending and the stretching modes during early stages of the dissociation process. At later times ($t>40$ fs), the activity along θ becomes significant leading to fast dissociation. The origin of the recurrences is also very clearly illustrated in Figs. 14(e) and 14(f). They seem to be arising due to the reentering or "leaking" of a small portion of the wave packet into the Franck–Condon region on its way out to the dissociative channels. Thus, the course of the dissociation process is very clearly depicted in these pictures, especially the increase in θ angle during the fragmentation of the molecule and the origin of recurrence features responsible for the fine structures in the spectrum.

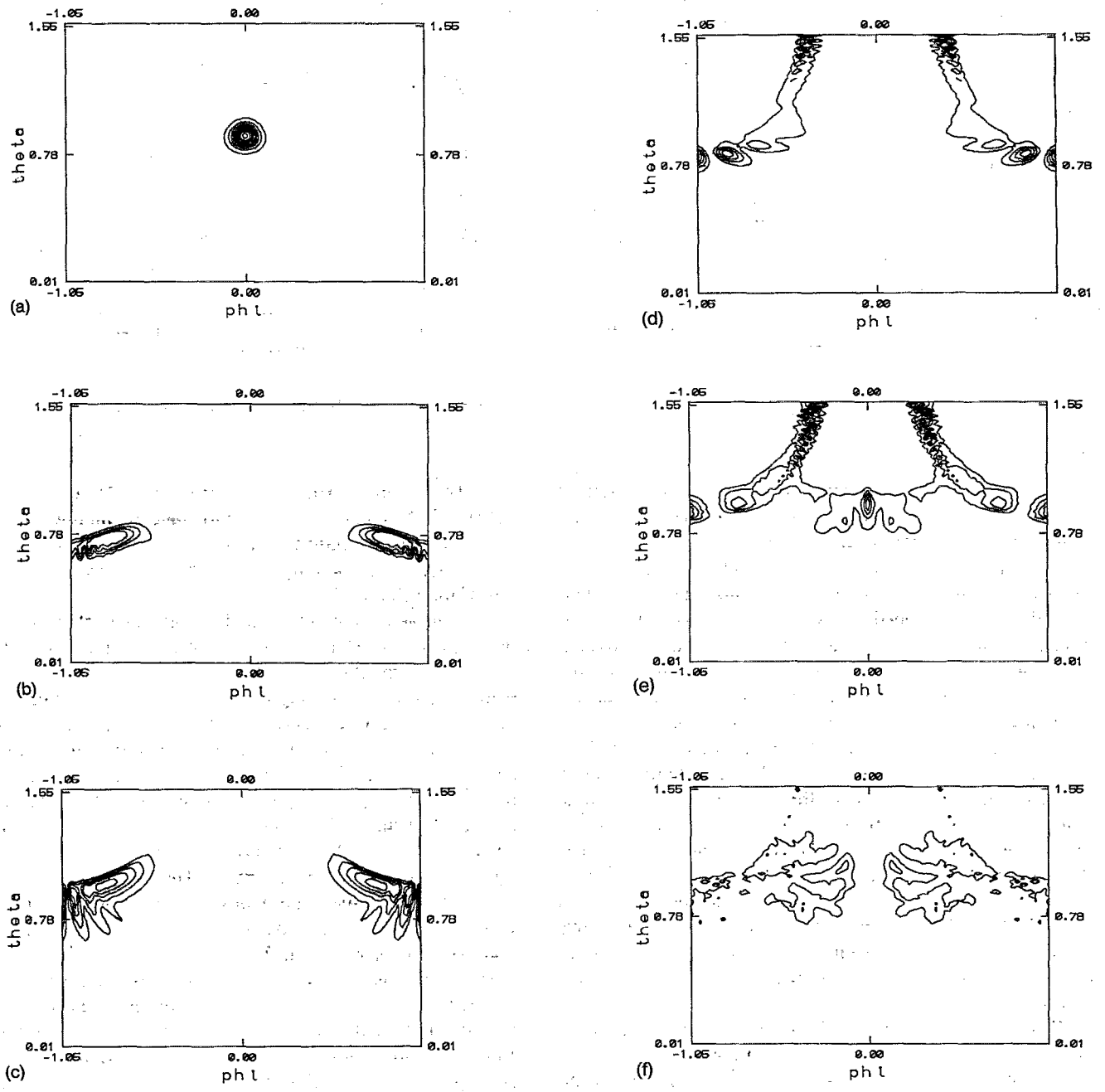

FIG. 14. Contour plots of the probability density as a function of θ and ϕ (in radians) at different time intervals t=0, 20, 40, 60, 80, and 120 fs in (a)–(f). The ρ dependence of the wave function has been integrated out.

VIII. SUMMARY AND CONCLUSION

We have carried out a detailed 3D study of ozone photodissociation dynamics in the Hartley absorption region using time-dependent wave packet methods. The initial wave function of the molecule before photon absorption has been directly discretized in the bond coordinates R_1, R_2, and β. The necessary transformation between these coordinates and hyperspherical coordinates has been introduced and the dynamics performed in the latter coordinate system. The use of hyperspherical coordinates fully explored the symmetry of the molecule and greatly simplified the numerical complexity of the problem. Two different PESs have been employed in the present study. We have carried out extensive convergence tests on the SW PES before the computed correlation function is compared with the experimental equivalent. Our converged calculations for J=0 on the SW PES reproduced successfully the characteristic recurrences in the experimentally derived correlation function. Particularly, the magnitude of the calculated correlation function is in very good agreement with the experimental counterpart. The absorption spectrum, obtained as the Fourier transform of the autocorrelation function showed near quantitative agreement with the experimen-

tal spectrum of Freeman *et al.* To the best of our knowledge, this is the first time the Hartley absorption spectrum is so well characterized by any theoretical calculations. The YM surface showed about a factor of 5 more recurrence intensity in the correlation function compared to that on the SW PES and the experimental. It is difficult to find a good explanation for this as our finding is in good agreement with the results of Yamashita *et al.*[8] who employed a completely different methodology in their calculations. The YM surface also exhibited a different convergence property with respect to the angular grids compared to the SW PES.

The effect of J on the recurrence behavior was examined by carrying out a calculation for $J=10$ on the SW PES within a planar approximation. The result of this calculation is nearly identical to that of $J=0$ demonstrating that the J effect is only of minor importance in the context of comparing the computed spectra with the experimental spectrum of Freeman *et al.*

We have also gathered important insight into the dissociation process by examining the time-evolving wave packet at different time intervals, which clearly illustrated the importance of including all three degrees of freedom in the calculation. Though the calculations reported in this paper were quite expensive (each converged wave packet propagation required about 9 h of CPU on a CRAY C92 supercomputer), we believe that the present dynamical investigation has provided a clear answer to some of the longstanding speculations regarding the discrepancy between the existing calculations and the experimental results.

ACKNOWLEDGMENTS

We thank Dr. K. Weide for many useful comments on the original version of this manuscript. This research is supported by the Danish Natural Science Research Council.

[1] P. J. Hay, R. T Pack, R. B. Walker, and E. J. Heller, J. Phys. Chem. **86**, 862 (1982).
[2] M. G. Sheppard and R. B. Walker, J. Chem. Phys. **78**, 7191 (1983).
[3] O. Atabek, M. T. Bourgeois, and M. Jacon, J. Chem. Phys. **84**, 6699 (1986).
[4] D. Chasman, D. J. Tannor, and D. G. Imre, J. Chem. Phys. **89**, 6667 (1988).
[5] B. R. Johnson and J. L. Kinsey, J. Chem. Phys. **91**, 7638 (1989).
[6] F. Le Quéré and C. Leforestier, J. Chem. Phys. **92**, 247 (1990).
[7] F. Le Quéré and C. Leforestier, J. Chem. Phys. **94**, 1118 (1991).
[8] K. Yamashita, K. Morokuma, F. Le Quéré, and C. Leforestier, Chem. Phys. Lett. **191**, 515 (1992).
[9] D. E. Freeman, K. Yoshino, J. R. Esmond, and W. H. Parkinson, Planet. Space Sci. **32**, 239 (1984).
[10] C. Lanczos, J. Res. Natl. Bur. Stand. **45**, 225 (1950).
[11] T. J. Park and J. C. Light, J. Chem. Phys. **85**, 5870 (1986).
[12] A. Barbe, C. Secroun, and P. Jouve, J. Mol. Spectrosc. **49**, 171 (1974).
[13] B. R. Johnson, J. Chem. Phys. **79**, 1916 (1983).
[14] J. T. Muckerman, R. D. Gilbert, and G. D. Billing, J. Chem. Phys. **88**, 4779 (1988); G. D. Billing, and J. T. Muckerman, J. Chem. Phys. **91**, 6830 (1989).
[15] R. Kosloff, J. Phys. Chem. **92**, 2087 (1988).
[16] D. Neuhauser and M. Baer, J. Chem. Phys. **90**, 4351 (1989).
[17] E. J. Heller, J. Chem. Phys. **68**, 2066 (1978); Acc. Chem. Res. **14**, 368 (1981).
[18] N. Marković and G. D. Billing, Chem. Phys. **173**, 385 (1993).